Avrupa Bilim ve Teknoloji Dergisi
Özel Sayı, S. 322-331, Eylül 2020

Araştırma Makalesi

www.ejosat.com ISSN:2148-2683

European Journal of Science and Technology
Special Issue, pp. 322-331, September 2020

Research Article

Discrete Time State Estimation with Kalman Filter and Adaptive LQR Control of a Time Varying Linear System

Mehmet Latif Levent[1*], Ömer Aydoğdu[2], Cüneyt Yücelbaş[3]

[1] Hakkari University, Faculty of Engineering, Electrical and Electronics Engineering, Hakkari, Turkey (ORCID: 0000-0002-7185-9029)
[2] Konya Technical University, Faculty of Engineering and Natural Sciences, Electrical and Electronics Engineering, Konya, Turkey (ORCID: 0000-0003-0815-0356)
[3] Hakkari University, Faculty of Engineering, Electrical and Electronics Engineering, Hakkari, Turkey (ORCID: 0000-0002-4005-6557)

(1st International Conference on Computer, Electrical and Electronic Sciences ICCEES 2020 – 8-10 October 2020)

(**DOI:** 10.31590/ejosat.804741)

ATIF/REFERENCE: Levent, M.L., Aydoğdu, Ö. & Yücelbaş, C. (2020). Discrete Time State Estimation with Kalman Filter and Adaptive LQR Control of a Time Varying Linear System. *European Journal of Science and Technology*, (Special Issue), 322-331.

Abstract

In this study, a new adaptive controller design was created that compensates for variable load effects and provides high control performance. In the proposed control method, Discrete Time Kalman Filter method (DKF), which estimates system output states, and Discrete Time Linear Quadratic Regulator (DLQR) method, one of the optimal control methods, were used. Although the DLQR control method produces good results when applied to unvarying systems, it cannot provide the desired response in time varying systems because it has no adaptation mechanism. In order to solve this problem, an adaptation mechanism based lyapunov method which has been developed that adapts to different environmental conditions, constantly updating a new state feedback gain matrix value (K_{new}) and optimal lyapunov adaptation gain values (γ_1 , γ_2 , γ_3 , γ_4 , γ_5 and γ_6) used for system control block such as position (x_1) control, speed (x_2) control and current (x_3) control. In this mechanism, lyapunov adaptation gain initial values were calculated using the Artificial Neural Network (ANN) method as a new approach. Thus, it was aimed to eliminate the variable load effects and to increase the stability of the system. In order to demonstrate the effectiveness of the proposed method, a variable loaded VsimLabs (Virtual Simulation laboratories) servo system was modelled as a time-varying linear system and used in practical implementation and simulation in Matlab-Simulink environment. Based on the experimental results and performance measurements such as Integral Square Error (ISE), Integral Absolute Error (IAE) and Integral time absolute error (ITAE), it was observed that the proposed method increases the system performance and stability by minimizing variable load effect and steady state error.

Keywords: Adaptation mechanism, Artificial neural network, Lyapunov method, Time varying linear system.

Kalman Filtresi ile Ayrık Zamanlı Durum Tahmini ve Zamanla Değişen Doğrusal Bir Sistemin Adaptif LQR Kontrolü

Öz

Bu çalışmada, değişken yük etkilerini kompanze eden ve yüksek kontrol performansını sağlayan yeni bir adaptif denetleyici tasarımı gerçekleştirilmiştir. Öne sürülen kontrol metodunda, sistem çıkış durumlarını tahmin eden ayrık zamanlı kalman filtresi (Discrete Time Kalman Filter, DKF) ve optimum kontrol yöntemlerinden biri olan Ayrık Zamanlı Doğrusal Kuadratik Regülator (Discrete Time Linear Quadratic Regulator, DLQR) metodlarından yararlanılmıştır. DLQR kontrol metodu zamanla yükü değişmeyen sistemlere tüm periyotlarda uygulandığında iyi sonuçlar üretmesine rağmen, adaptasyon mekanizması bulunmadığından, zamanla değişen sistemlerde istenilen cevabı verememektedir. Bu problemi çözmek için, farklı çevre ortamlarına uyum sağlayan, yeni bir durum geri besleme kazanç matrix değerini (K_{new}) ve pozisyon (position, x_1) kontrol, hız (speed, x_2) kontrol ve akım (current, x_3) kontrol gibi sistem kontrol blokları için kullanılan optimum lyapunov adaptasyon kazanç değerlerini (γ_1 , γ_2 , γ_3 , γ_4 , γ_5 ve γ_6) sürekli güncelleyen bir lyapunov tabanlı adaptasyon mekanizması yöntemi geliştirilmiştir. Bu mekanizmada lyapunov adaptasyon kazancın başlangıç değerleri, tasarımda yeni bir yaklaşım olarak Yapay Sinir Ağı (Artificial Neural Network, ANN) metodu ile

[*] Corresponding Author: Hakkari University, Faculty of Engineering, Electrical and Electronics Engineering, Hakkari, Turkey, ORCID: 0000-0002-7185-9029, mehmetlatiflevent@hakkari.edu.tr

hesaplanmıştır. Böylece değişken yük etkilerinin minimize edilmesi ve sistem kararlılığının artırılması amaçlanmıştır. Önerilen yöntemin etkinliğini pratik uygulama ve simülasyonda göstermek için, zamanla değişen doğrusal bir sistem olan değişken yüklü bir Sanal Simülasyon laboratuvarları (Virtual Simulation Laboratories, VsimLabs) servo sistemi modellenmiş ve Matlab Simulink ortamında kullanılmıştır. Deneysel sonuçlara ve İntegral Karesel Hata (Integral Square Error, ISE), İntegral Mutlak Hata (Integral Absolute Error, IAE), İntegral Zamanlı Mutlak Hata (Integral time absolute error, ITAE) gibi performans ölçümlerine göre, önerilen yöntemin değişken yük etkisini ve sürekli durum hatasını minimize ederek sistem performans ve kararlılığını artırdığı görülmüştür.

Anahtar Kelimeler: Adaptasyon Mekanizması, Yapay Sinir Ağı, Lyapunov Yöntemi, Zamanla Değişen Doğrusal Sistem.

1. Introduction

Motors are used in robotic applications, manipulators, washing machines, dryers, electronic items used in the kitchen and in many domestic applications. Therefore, Direct Current (DC) motors are frequently preferred in industrial and many engineering applications. Although the brushed and brushless permanent magnet motors are meeting certain motor requirements such as having low voltage limits, being affordable, being easy to control, and being supplied rapidly, in recent years, the costs of the brushed dc motors, which are among the basic elements of power electronics, are decreasing and they protect their place to an important extent within the international market [1-2].

Basic Kalman Filter can only be applied to linear random systems by nature [3]. Accordingly, the Kalman filters are expressed as the mathematical method that can minimize the disruptive effects and estimate the states by reducing the root-mean-square error. This filter structure is especially used in space and military technology [4], robotics and trajectory control applications [5], hybrid tracking technique [6], dynamic data processing [7], navigation sensors data fusion [8], Mobile Radio Link Adaptation by Radio Channel State Prediction [9], artificial neural networks [10], and different hybrid controller designs [11]. Accurately estimating the dynamic states (such as position, speed, and current) of a system such as a DC Motor is a very important element in terms of system stability [12]. In previous studies, it is concluded that Kalman Filter structures play an important role in optimally estimating system states. For instance, study in [13], noise-free unknown states were estimated using a discrete Kalman Filter and a successful control of the system was achieved.

The LQR approach, which is one of the modern control methods that improves system performance, is frequently used in the literature for optimal control problems [14]. In control of state-feedback systems, an observer such as the Kalman Filter must be used in order for the states to be used in conjunction with the DLQR controller. Because in the DLQR method, the states of the system are needed to generate the control signal. The basic working principle of this method is to minimize the quadratic performance index [15].

The Lyapunov stability criteria and MIT rule are frequently used methods in designing traditional adaptive control systems to increase system stability. This method organizes the parameter values based on reference model output value, and intends to increase the system performance against the disruptive effects. The Lyapunov based adaptive control method that is generally more effective on the system performance, and it is preferred in different fields and control mechanisms. Among the applications as the examples of usage area of the Lyapunov-based adaptive control method are position control of permanent magnet synchronous motor[16], X-Y table experimental platforms control [17-18], DC motor speed control [19], and design of a stable and robust tension controller [20].

2. Modelling of the VsimLabs Servo System

As is seen in Figure 1, a VSimLabs servo system that can alter the load in time was used in the simulations. In engineering applications, brushed DC motors is widely used as an actuator for electromechanical energy conversion. The VLS system actuated with brushed DC motor, which has the electric circuit of the armature, and the variable loaded body diagram of the rotor are shown in Figure 1. VLS plant and brushed DC motor parameters are given in Table 1. The following differential equations can be written based on the Newton's law together with the Kirchhoff's law from the Figure 1;

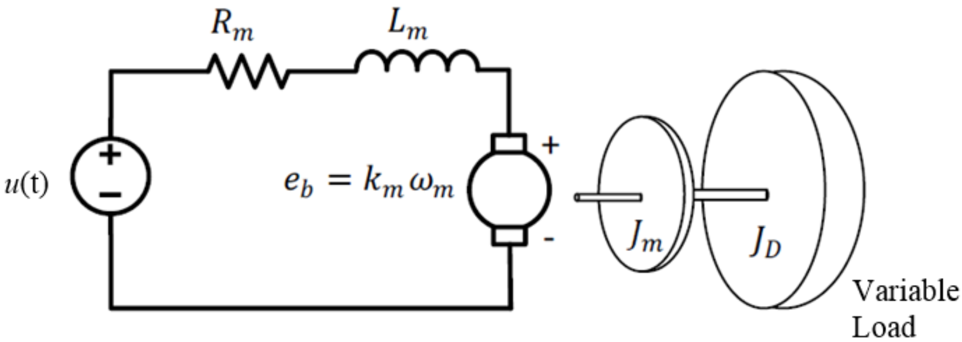

Fig. 1 Equivalent circuit of the VLS system.

$$u(t) = R_a i(t) + L_a \frac{di(t)}{dt} + e_b(t). \tag{1}$$

$$\tau_m(t) = J_m \frac{d\omega_m(t)}{dt} + B_m\omega_m(t) + \tau_l(t). \tag{2}$$

$$\omega_m(t) = \frac{d\theta_m(t)}{dt}. \tag{3}$$

where; $i(t)$ is the armature current, $e_b(t)$ is the back EMF voltage, $\tau_m(t)$ is the produced motor torque, $\tau_l(t)$ is the load torque, $\theta_m(t)$ is the angle of the armature, $\omega_m(t)$ is the angular velocity of the armature. The motor torque $\tau_m(t)$ is related to the armature current $i(t)$ by a constant factor k_t, and the back EMF $e_b(t)$ is related to the rotational velocity of the armature $\omega_m(t)$ by a constant factor $k_m(t)$, as given by the following equations;

$$\tau_m(t) = k_t i(t) \tag{4}$$

$$e_b(t) = k_m\omega_m(t). \tag{5}$$

In the VLS system, equivalent armature load torque $\tau_l(t)$ may be expressed as:

$$\tau_l(t) = J_l \frac{d\omega_m(t)}{dt} + B_l\omega_m(t). \tag{6}$$

If (6) is substituted in (2), the general moment expression for the motor is obtained as follows.

$$\tau_m(t) = (J_m + J_l)\frac{d\omega_m(t)}{dt} + (B_m + B_l)\omega_m(t). \tag{7}$$

The following equations are obtained for the state space expression of the system by using (1), (3)–(5), and (7):

$$\frac{di(t)}{dt} = -\frac{R_a}{L_a}i(t) - \frac{k_b}{L_a}\omega_m(t) + \frac{1}{L_a}u(t), \tag{8}$$

$$\frac{d\omega_m(t)}{dt} = \frac{k_t}{J_{eq}}i(t) - \frac{B_{eq}}{J_{eq}}\omega_m(t), \tag{9}$$

$$\frac{d\theta_m(t)}{dt} = \omega_m(t), \tag{10}$$

Table 1. VLS plant and brushed DC motor parameters

Symbol	Definition	Value
$u(t)$	Nominal Voltage	$12V$
R_a	Motor armature resistance	2.9Ω
L_a	Motor armature inductance	$0.278mH$
k_t	Motor torque constant	$0.0256\ Nm/A$
k_b	Motor back-EMF constant	$0.0256\ \mathrm{V}/(rad/s)$
J_m	Motor inertia	$1.49\times10^{-6}\,kgm^2$
B_m	Motor viscous coefficient	$7\times10^{-6}\,Nms$
m_d	Mass of Load On Disk	$0.068\ kg$
r_d	Disk Load Radius	$0.025\ m$
J_d	Disk inertia	$2.125\times10^{-5}\,kgm^2$

J_d shows the total inertia moment acting on the motor shaft. The inertia moment of a disk with a mass of m and a radius of r with reference to its own axis of rotation is calculated through $J = \frac{1}{2}mr^2$. The total inertia of the system is comprised of the rotor of the DC motor and the load in the form of a disk. Since the load is also directly connected to the motor shaft, the total inertia moment of the system is obtained through the equation $J_{eq} = J_m + J_d + J_l$. Here J_l refers to the inertia moment created by variable loads. At the same time, $B_{eq} = B_m + B_l$ is obtained due to variable loads. If (8)–(10) are arranged in state space model and armature angle is accepted as the output, the state space expression of the servo system is obtained as (11) and (12):

$$\frac{dx(t)}{dt} = Ax(t) + Bu(t), \tag{11}$$

$$y(t) = Cx(t), \tag{12}$$

where; state variables are defined as;

$$x(t) = \begin{bmatrix} x_1(t) \\ x_2(t) \\ x_3(t) \end{bmatrix} = \begin{bmatrix} \theta_m(t) \\ \omega_m(t) \\ i_1(t) \end{bmatrix}, \tag{13}$$

and the state, input and output matrices are obtained as;

$$A = \begin{bmatrix} 0 & 1 & 0 \\ 0 & -\frac{B_{eq}}{J_{eq}} & \frac{k_t}{J_{tot}} \\ 0 & -\frac{k_b}{L_a} & -\frac{R_a}{L_a} \end{bmatrix}, \qquad B = \begin{bmatrix} 0 \\ 0 \\ \frac{1}{L_a} \end{bmatrix}, \qquad C = \begin{bmatrix} 1 & 0 & 0 \end{bmatrix}.$$

3. Discrete Time Kalman Filter and Adaptive LQR Control

The Discrete time kalman filter and adaptive LQR control structure is given in Figure 2 below. Our main goal in this study is to ensure that the system adapts to different environmental conditions by constantly updating the state feedback gain matrix value (K_{new}). In order to obtain the output value, in other words the K_{new} matrix, in the Lyapunov stability criterion based adaptation mechanism shown in Figure 3, four input values are used as reference signal, the system output states estimated by the discrete Kalman Filter, Klqr matrix calculated through the discrete Riccati Equation, and control input. In the system, different adaptation blocks for the states that are position (x_1), speed (x_2) and current (x_3) are designed.

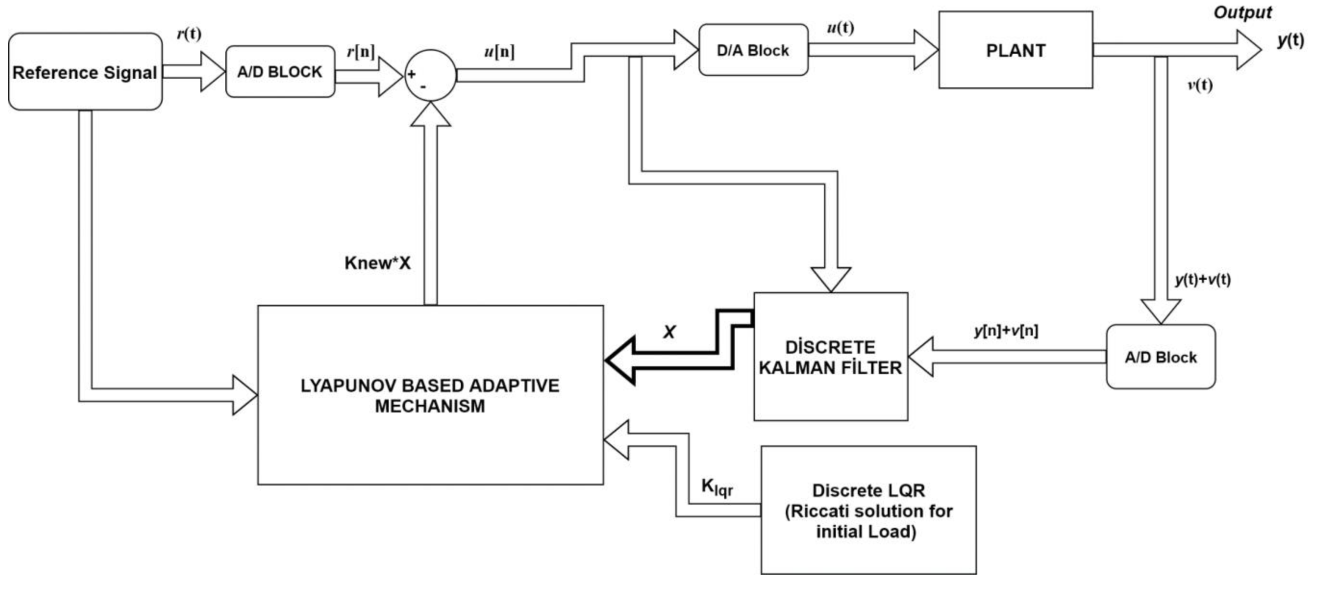

Fig. 2 Discrete Time Kalman Filter and Adaptive LQR Control Block Diagram

The first block provides position control; the second block provides speed control and the third block provides adaptation for the current control. Reference input $r(t)$ is used for the first block and reference input $wref$ data for the second block is defined as the output of the first block. Similarly, reference input $iref$ of the third block is defined as the output data of the second block. In this regard, the purpose of this research is to perform a new adaptive algorithm that ensures optimal state feedback of the system on variable loads. Feedback gain value (K_{new}) in this algorithm that is designed to fit for following equations varies based on the environment conditions.

If the gain matrix value at discrete LQR output and also the adaptively produced feedback gain value are respectively defined as $K_{lqr} = [a_1 \quad a_2 \quad a_3]$ and $K_{new} = [b_1 \quad b_2 \quad b_3]$; update equations of the new adaptive gain matrix value are obtained by using adaptive u_1, u_2 and u_3 values as follows.

$$b_1 = a_1 - \frac{u_1}{x_1}. \quad (14)$$

$$b_2 = a_2 - \frac{u_2}{x_2}. \quad (15)$$

$$b_3 = a_3 - \frac{u_3}{x_3}. \quad (16)$$

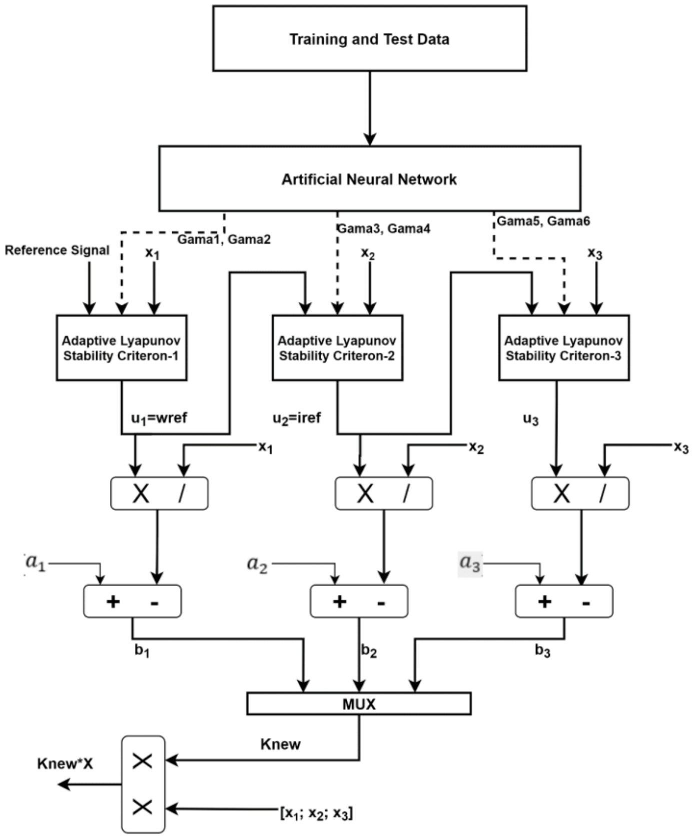

Fig. 3 Lyapunov stability criterion based adaptation mechanism

Hereby, the adaptive u_1, u_2 and u_3 values are separately obtained via model reference adaptive control approach by utilizing the reference model defined. u_1 adaptive output reference is obtained; the similar steps are also applied for u_2 and u_3 outputs [21]. As is understood from study in [22], the Lyapunov function needs to be higher than zero for the system to be stable. Additionally, the derivative of the same function needs to be smaller than zero. Below equations can be obtained when the derivative of lyapunov function is taken;

$$\frac{dv}{dt} = -a_m e^2 - (b\theta_2 + a - a_m)\left(\frac{d\theta_2}{dt} - \gamma_1 ye\right) + \frac{1}{\gamma_2}(b\theta_1 - b_m)\left(\frac{d\theta_1}{dt} + \gamma_2 re\right). \quad (17)$$

By reference to Equation 17, the derivative expression of the function becomes smaller than zero if the parameter values are obtained. Accordingly, the stability condition of the system is ensured, If the parameters are updated as follows;

$$\frac{d\theta_1}{dt} = -\gamma_2 re. \quad (18)$$

$$\frac{d\theta_2}{dt} = \gamma_1 ye, \quad (19)$$

$$\theta_1 = \frac{-\gamma_2}{s} re, \quad (20)$$

$$\theta_2 = \frac{\gamma_1}{s} ye. \quad (21)$$

where θ_1 and θ_2 are the control parameters with adjustable gains γ_1 and γ_2. In conclusion, the system becomes stable if a proper controller design is provided in Equation 22 and Equation 23. However, it is needed to know the optimal values that provide the system to run more stable when the adjustement gain values are not known. In this study, the best adjustment gain (γ_1 , γ_2) values are actualized by using an artificial neural networks (ANN). it is used an ANN structure that has train function TRAINLM, adaption learning function LEARNGDM, performance function MSE, Feed-forward backpropagation as the network type, 16 hidden layers and 1 output layers. 200 data set for γ_1 and γ_2 gain values and IAE performance criteria as the training data and randomly produced 10000 values are were entered in the ANN algorithm as value test data. The same steps were performed for (γ_3 , γ_4) and (γ_5 , γ_6) .

The experimental system is given in Figure 4. This system includes a V-DAQ data acqusition board, DC Motor, variable loads, initial disk load, DAC-ADC board an PC.

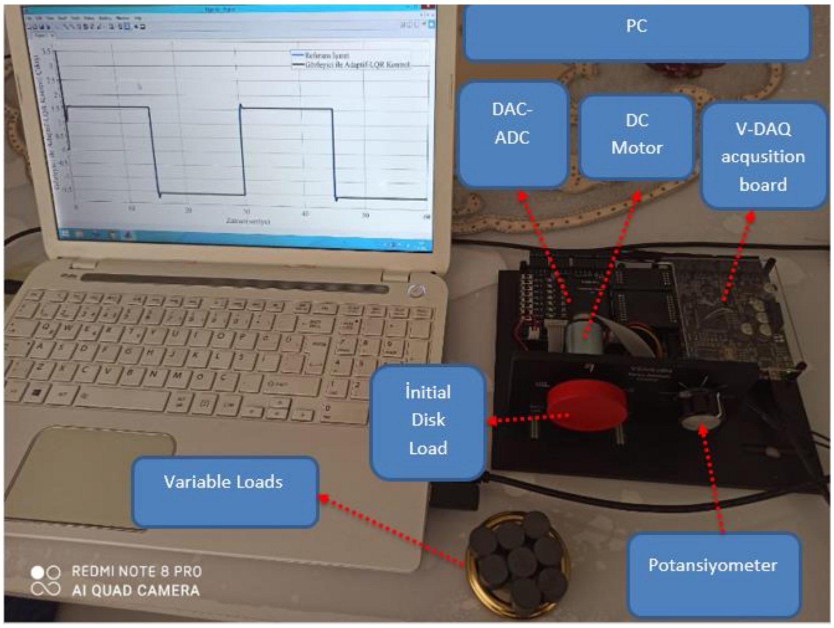

Fig. 4 A photograph of the experimental system.

4. Simulation and Experimental Results

In this section, both simulation and experimental results are discussed. Initially, the results of the methods applied to the unvarying VsimLabs servo system were compared in the Matlab/Simulink simulation environment. The total inertia expression ($J_{eq} = J_m + J_d$) of a constant-loaded motor was calculated. Here, J_m is the inertia of the rotor and J_d is the inertia of the disk. As per the expression of the inertia of the disk, it is calculated through the equation $J_d = 0.5 \times m_d \times r_d^{\,2}$. In this equation, m_d represents the mass of the disk and r_d represents the radius of the disk. When referencing Table 1, the value $J_{tot} = 2.098 \times 10^{-5}$ was applied in all periods without any changes. Subsequently, the varying load ($J_{eq} = J_m + J_d + J_l$) was added to the VsimLabs servo system after the 7th second, and the equation was updated as $J_{eq} = 1.08 \times 10^{-2}$. After adding the variable load, the output curves and parameter changes of discrete time Kalman Filter and adaptive LQR control methods were obtained.

In this case the VLS system parameters discrete time A_k , B_k and C_k are obtained as:

$$A_k = \begin{bmatrix} 1 & 0.001 & 10^{-4} \\ 0 & 0.9854 & 0 \\ 0 & -0.0087 & 0.001 \end{bmatrix}, \quad B_k = \begin{bmatrix} 0.0002 \\ 0.3780 \\ 0.3418 \end{bmatrix}, C_k = \begin{bmatrix} 1 & 0 & 0 \end{bmatrix}.$$

Also, if we choose the R and Q parameters for the discrete kalman filter and discrete LQR as follows, the LQR gain is found as;

$$K_{lqr} = \begin{bmatrix} 1.1147 & 1.0794 & 0.1264 \end{bmatrix}, \; Q = \begin{bmatrix} 3 & 0 & 0 \\ 0 & 3 & 0 \\ 0 & 0 & 3 \end{bmatrix}, \; R{=}1,$$

In the design of the Lyapunov based adaptive control system a 2nd order system given in Equation 22 is used as a reference model. Here, the reference model has been created in accordance with both settle time and maximum overshoot. After completing successful simulation works, the same steps were applied on the experiment set. The system output and parameter change curves are discussed in Section 4.2.

$$G_m(s) = \frac{40000}{(s+200-i)(s+200+i)} = \frac{40000}{\left(s^2+400s+40001\right)}. \tag{22}$$

4.1. Simulation Results

When adaptive LQR and discrete kalman filter with DLQR control methods for unvarying system are applied, the result are shown in Figure 5. Examining zoom area shown in Figure 6, it is concluded that the position output signal rapidly catches the reference signal. As is shown in Table 2, comparing the results based on the performance measurements, it is understood that the proposed system produces better results and has a high performance.

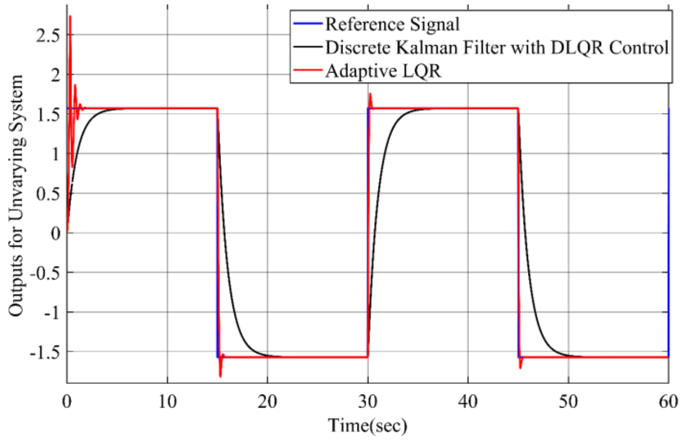

Fig. 5 Proposed Control Method in Unvarying System

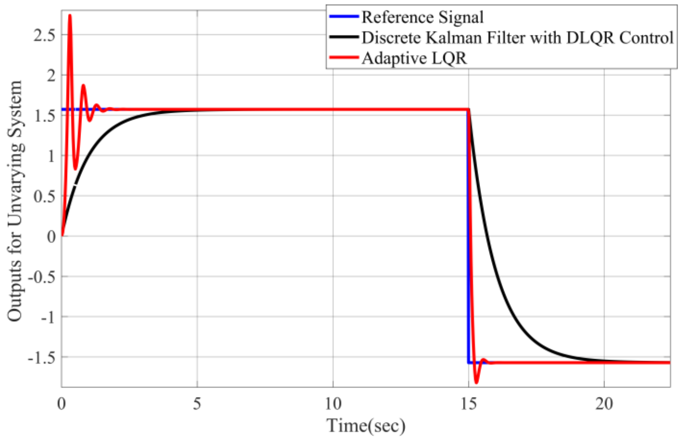

Fig. 6 Zoom Area in Figure 5

One of the most remarkable characteristics of the proposed control method is to compensate the effects such as variable load. The response curves obtained after adding the variable load to the system at the 6.8th second are shown in the Figure 7 and Figure 8.

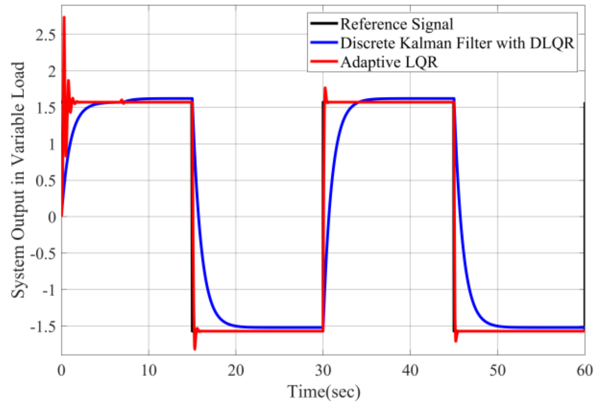

Fig. 7 Proposed Control Method in Variable Load

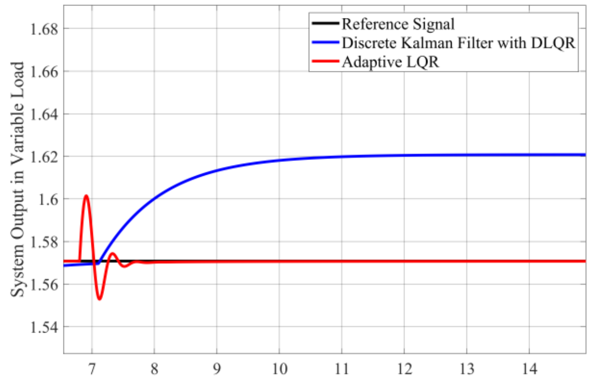

Fig. 8 Zoom Area in Figure 7

4.2. Experimental Results

For a unvarying servo system, experimental application results of the proposed method are shown in the Figure 9. Examining Figure 10, it is seen that the adaptive LQR control system output quickly settles into the reference input signal, with decreasing oscillations in subsequent periods. The system response curve, when the variable load effect takes place, is shown in the Figure 11.

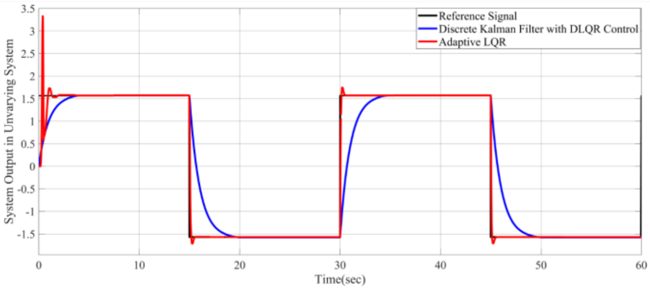

Fig. 9 Proposed Control Method in Unvarying System

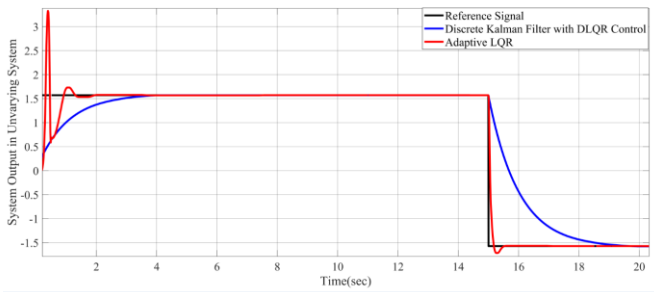

Fig. 10 Zoom Area in Figure 9

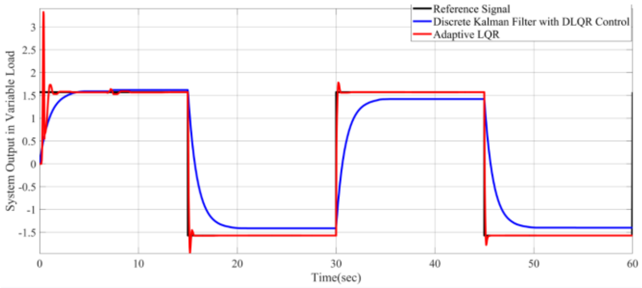

Fig. 11 Proposed Control Method in Variable Load

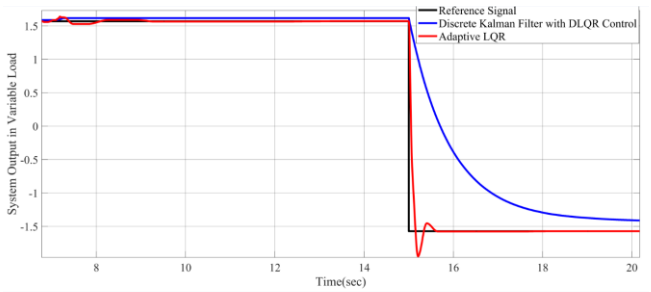

Fig. 12 Zoom Area in Figure 11

Through the proposed method, the load effect is quickly compensated. However, in the discrete Kalman Filter with DLQR control method response curve, it was observed that the system output signal moves away from the desired reference signal due to the effect of variable load. In the adaptive mechanism, which was designed using reference signal, control input, and system states, changes in Lyapunov parameters updated to adapt to different environmental conditions are shown in the figures below. In addition, the new adaptive gain matrix value (K_{new}) is shown in Figure 19 and Figure 20.

Table 2. Performance Measurement

Unvarying Servo System	**ISE**	**IAE**	**ITAE**	***Variable Loaded Servo System***	**ISE**	**IAE**	**ITAE**
Simulation Results				***Simulation Results***			
LQR Control Method	15.93	10.9	291.1	LQR Control Method	16.38	12.98	362.7
Adaptive LQR System	1.779	1.300	19.51	Adaptive LQR System	1.775	1.306	19.57
Experimental Results				***Experimental Results***			
LQR Control Method	15.63	2.098	2.098	LQR Control Method	16.45	17.04	520.9
Adaptive LQR System	2.057	1.598	18.46	Adaptive LQR System	2.098	1.703	19.87

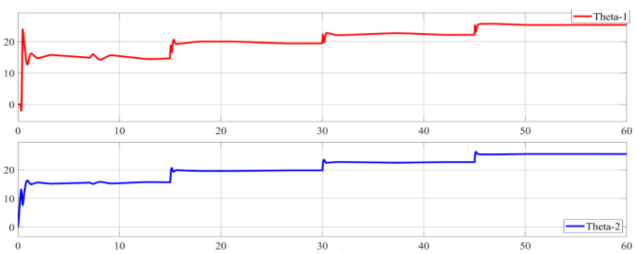

Fig. 13 Change of θ_1 and θ_2

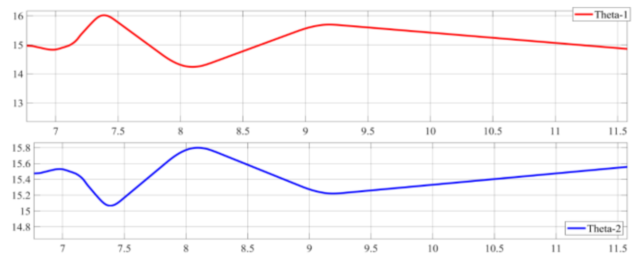

Fig. 14 After t=6.8 seconds for figure 13

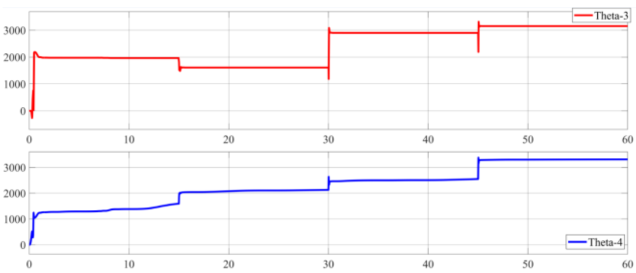

Fig. 15 Change of θ_3 and θ_4

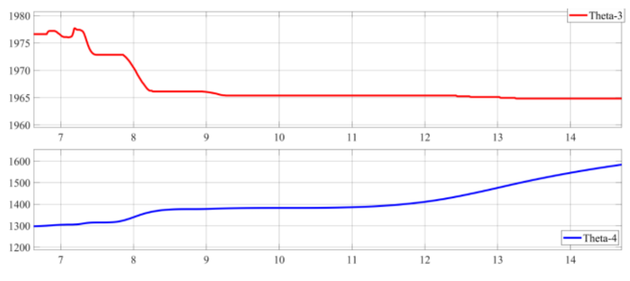

Fig. 16 After t=6.8 seconds for figure 15

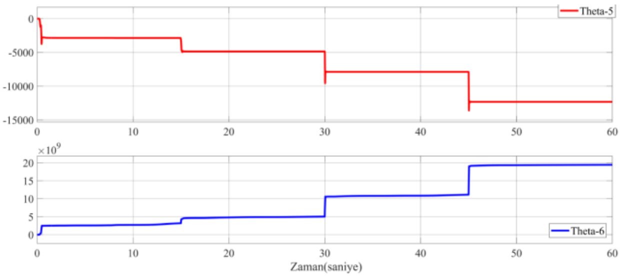

Fig. 17 Change of θ_5 and θ_6

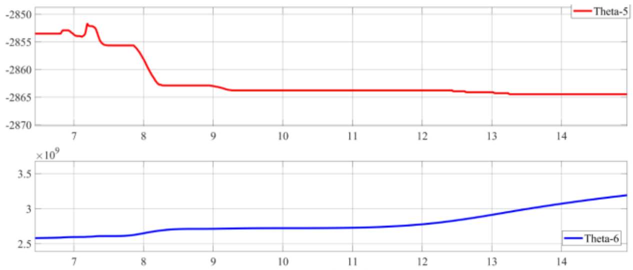

Fig. 18 After t=6.8 seconds for figure 17

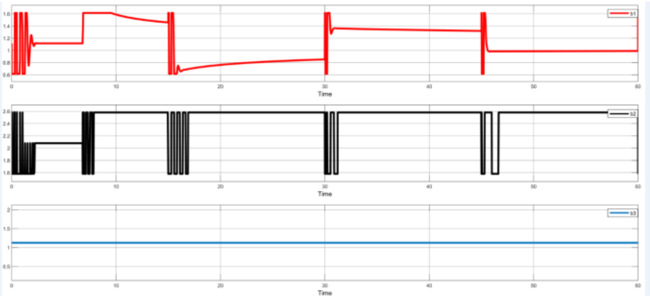

Fig. 19 Change of θ_5 and θ_6

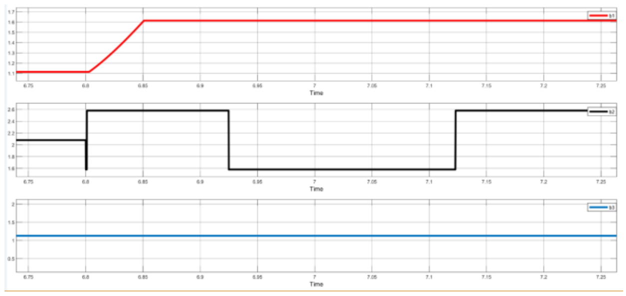

Fig. 20 After t=6.8 seconds for figure 19

4. Conclusions

The new control method with discrete time LQR and kalman filter based adaptive state feedback control that compensates the disruptive effects and also increases the system performance was designed in this research. This controller structure was successfully used in control of VSimLabs servo system that can change the load over time. As is known, it is not possible to completely remove the disruptive effects. The system can estimate the states of variable loaded servo system, thus, the disruptive effects can be minimized. It is observed on experimental and simulation results that the proposed method compensates well in time-varying systems; so, the system is beneficial in optimal controlling of the system. It is understood from the system results that the system control parameters can adapt itself in time.

5. Acknowledge

This work was supported by Research Fund of the Hakkari University. Project Number: FM20BAP11.

References

[1] Roy, T. K., Pervej, M. F., Tumpa, F. K., & Paul, L. C. (2016, December). Nonlinear adaptive controller design for velocity control of a DC motor driven by a DC-DC buck converter using backstepping approach. In 2016 2nd International Conference on Electrical, Computer & Telecommunication Engineering (ICECTE) (pp. 1-4). IEEE.

[2] Afjei, E., Ghomsheh, A. N., & Karami, A. (2007, September). Sensorless speed/position control of brushed DC motor. In 2007 International Aegean Conference on Electrical Machines and Power Electronics (pp. 730-732). IEEE.

[3] Bishop G, Welch G. An introduction to the kalman filter. Chapel Hill, NC, USA: Proc of SIGGRAPH, 2001.J. Breckling, Ed., The Analysis of Directional Time Series: Applications to Wind Speed and Direction, ser. Lecture Notes in Statistics. Berlin, Germany: Springer, 1989, vol. 61.

[4] Teixeira BO, Santillo MA, Erwin RS, Bernstein DS. Spacecraft tracking using sampled-data Kalman filters. IEEE Control Systems Magazine 2008; 28 (4): 78-94.

[5] Haixia Q, Banhazi TM, Zhigang Z, Low T, Brookshaw IJ. Preliminary laboratory test on navigation accuracy of an autonomous robot for measuring air quality in livestock buildings. International Journal of Agricultural and Biological Engineering 2016; 9 (2): 29-39.

[6] Artemciukas E, Sakalauskas L, Zulkas E. Kalman filter for hybrid tracking technique in augmented reality. Elektronika ir Elektrotechnika 2016; 22 (6): 73-79 .

[7] Kluga A, Kluga J. Dynamic Data Processing with Kalman Filter. Elektronika ir Elektrotechnika 2011; 111 (5): 33-36.

[8] Bistrovs V, Kluga A. The analysis of the UKF-based navigation algorithm during GPS outage. Elektronika ir Elektrotechnika 2013; 19 (10): 13-16.

[9] Ziacik P, Wieser V. Mobile radio link adaptation by radio channel state prediction. Elektronika ir Elektrotechnika 2011; 114 (8): 27-30

[10] Castaneda C, Loukianov A, Sanchez E, Castillo-Toledo B. Real-time torque control using discrete-time recurrent high-order neural networks. Neural Computing and Applications 2013; 22 (6): 1223-1232.

[11] Castaneda CE, Loukianov AG, Sanchez EN, Castillo-Toledo B. Discrete-time neural sliding-mode block control for a DC motor with controlled flux. IEEE Transactions on Industrial Electronics 2011; 59 (2): 1194-1207.

[12] Akhlaghi, S., Zhou, N., & Huang, Z. (2017, July). Adaptive adjustment of noise covariance in Kalman filter for dynamic state estimation. In 2017 IEEE power & energy society general meeting (pp. 1-5). IEEE.

[13] Ali, D., Asim, M., Wallam, F., Abbas, A., & Naudhani, Y. (2019, January). Experimental testing of observers comprising discrete Kalman filter and high-gain observers. In 2019 2nd International Conference on Computing, Mathematics and Engineering Technologies (iCoMET) (pp. 1-5). IEEE.

[14] Abut, T. (2016). Modeling and Optimal Control of a DC Motor. Int. J. Eng. Trends Technol, 32(3), 146-150.

[15] Aravind, M. A., Saikumar, N., & Dinesh, N. S. (2017, May). Optimal position control of a DC motor using LQG with EKF. In 2017 international conference on mechanical, system and control engineering (ICMSC) (pp. 149-154). IEEE.

[16] Lin FJ, Sun IF, Yang KJ, Chang JK. Recurrent fuzzy neural cerebellar model articulation network fault-tolerant control of six-phase permanent magnet synchronous motor position servo drive. IEEE Transactions on Fuzzy Systems 2015; 24 (1): 153-167.

[17] Wang H, Zhao X, Tian Y. Trajectory tracking control of XY table using sliding mode adaptive control based on fast double power reaching law. Asian Journal of Control 2016; 18 (6): 2263-2271.

[18] Mao WL, Hung CW, Suprapto. Adaptive fuzzy trajectory control for biaxial motion stage system. Advances in Mechanical Engineering 2016; 8 (4) 1-16.

[19] Rashidi B, Esmaeilpour M, Homaeinezhad MR. Precise angular speed control of permanent magnet DC motors in presence of high modeling uncertainties via sliding mode observer-based model reference adaptive algorithm Mechatronics 2015; 28: 79-95.

[20] Talian P, Perdukova D, Fedor P. Stable and Robust Tension Controller for Middle Section of Continuous Line. Elektronika ir Elektrotechnika 2018; 24 (1): 3-10.

[21] Aydogdu, O., & Levent, M. L. (2019). Kalman state estimation and LQR assisted adaptive control of a variable loaded servo system. Engineering, Technology & Applied Science Research, 9(3), 4125-4130.

[22] Aydogdu, O., & Levent, M. L. (2020). State Estimation with Reduced-Order Observer and Adaptive-LQR Control of Time Varying Linear System. Elektronika ir Elektrotechnika, 26(2), 24-31.